Simeprevir suppresses SARS-CoV-2 replication and synergizes with remdesivir

Authors

Ho Sing Lo[1,*], Kenrie P. Y. Hui[2,*], Hei-Ming Lai[3,4,5,*], Khadija Shahed Khan[1], Simranjeet Kaur[6], Zhongqi Li[4,5], Anthony K. N. Chan[7], Hayley Hei-Yin Cheung[8], Ka Chun Ng[2], John Chi Wang Ho[2], Yu Wai Chen[9], Bowen Ma[1], Peter Man-Hin Cheung[10], Donghyuk Shin[11], Kaidao Wang[12], Kuen-Phon Wu[13], Ivan Dikic[11], Po-Huang Liang[13], Zhong Zuo[1], Francis K. L. Chan[4,14], David S. C. Hui[4,15], Vincent C. T. Mok[4,16], Kam-Bo Wong[8], Ho Ko[3,4,5,16,17], Wei Shen Aik[6], Michael C. W. Chan[2,†], Wai-Lung Ng[1,†]

Affiliations

[1]School of Pharmacy, Faculty of Medicine, The Chinese University of Hong Kong, Hong Kong
[2]School of Public Health, Li Ka Shing Faculty of Medicine, The University of Hong Kong, Hong Kong
[3]Department of Psychiatry, Faculty of Medicine, The Chinese University of Hong Kong, Hong Kong
[4]Department of Medicine and Therapeutics, Faculty of Medicine, The Chinese University of Hong Kong, Hong Kong
[5]Li Ka Shing Institute of Health Sciences, Faculty of Medicine, The Chinese University of Hong Kong, Hong Kong
[6]Department of Chemistry, Faculty of Science, Hong Kong Baptist University, Hong Kong
[7]Department of Systems Biology, Beckman Research Institute, City of Hope, Duarte, CA, USA
[8]School of Life Sciences, Centre for Protein Science and Crystallography, State Key Laboratory of Agrobiotechnology, Faculty of Science, The Chinese University of Hong Kong, Hong Kong
[9]Department of Applied Biology and Chemical Biology and the State Key Laboratory of Chemical Biology and Drug Discovery, The Hong Kong Polytechnic University, Hong Kong
[10]School of Public Health, Faculty of Medicine, The Chinese University of Hong Kong, Hong Kong
[11]Buchmann Institute for Molecular Life Sciences, Goethe University, Frankfurt am Main, Germany
[12]Protein Production Department, GenScript Biotech Corporation, Nanjing, China
[13]Institute of Biological Chemistry, Academia Sinica, Taipei, Taiwan
[14]Institute of Digestive Disease, Faculty of Medicine, The Chinese University of Hong Kong, Hong Kong
[15]Stanley Ho Center for Emerging Infectious Diseases, Faculty of Medicine, The Chinese University of Hong Kong, Hong Kong
[16]Gerald Choa Neuroscience Centre, Margaret K.L. Cheung Research Centre for Management of Parkinsonism, Faculty of Medicine, The Chinese University of Hong Kong, Hong Kong
[17]School of Biomedical Sciences, Peter Hung Pain Research Institute, Faculty of Medicine, The Chinese University of Hong Kong, Hong Kong

[*]These authors contributed equally to this work

[†]To whom correspondence should be addressed: M.C.W.C. (mchan@hku.hk) or W.L.N. (billyng@cuhk.edu.hk)

One Sentence Summary

Discovery of simeprevir as a potent suppressor of SARS-CoV-2 viral replication that synergizes remdesivir.

Abstract

The recent outbreak of coronavirus disease 2019 (COVID-19), caused by the severe acute respiratory syndrome coronavirus 2 (SARS-CoV-2) virus, is a global threat to human health. By *in vitro* screening and biochemical characterization, we identified the hepatitis C virus (HCV) protease inhibitor simeprevir as an especially promising repurposable drug for treating COVID-19. We also revealed that simeprevir synergizes with the RNA-dependent RNA polymerase (RdRP) inhibitor remdesivir to suppress the replication of SARS-CoV-2 *in vitro*. Our results provide preclinical rationale for the combination treatment of simeprevir and remdesivir for the pharmacological management of COVID-19 patients.

Keywords

Simeprevir, Remdesivir, SARS-CoV-2, COVID-19, Drug repurposing, Drug synergism

Introduction

The recent outbreak of infection by the novel betacoronavirus severe acute respiratory syndrome coronavirus 2 (SARS-CoV-2) has spread to almost all countries and claimed more than 260,000 lives worldwide (WHO situation report 107, May 6, 2020). Alarming features of COVID-19 include a high risk of clustered outbreak both in community and nosocomial settings, and up to one-fifth severe/critically ill proportion of symptomatic inpatients reported (*1*–*4*). Furthermore, a significant proportion of infected individuals are asymptomatic, substantially delaying their diagnoses, hence facilitating the widespread dissemination of COVID-19 (*5*). With a dire need for effective therapeutics that can reduce both clinical severity and viral shedding, numerous antiviral candidates have been under clinical trials or in compassionate use for the treatment of SARS-CoV-2 infection (*6*).

Several antivirals under study are hypothesized or proven to target the key mediator of a specific step in the SARS-CoV-2 viral replication cycle. For instance, lopinavir/ritonavir (LPV/r) and danoprevir have been proposed to inhibit the SARS-CoV-2 main protease (M^{pro}, also called $3CL^{Pro}$) needed for the maturation of multiple viral proteins; chloroquine (CQ) / hydroxychloroquine (HCQ) [alone or combined with azithromycin (AZ)] may abrogate viral replication by inhibiting endosomal acidification crucial for viral entry (*7*, *8*); nucleoside analogues such as remdesivir, ribavirin, favipiravir and EIDD-2801 likely inhibit the SARS-CoV-2 nsp12 RNA-dependent RNA polymerase (RdRP) and/or induce lethal mutations during viral RNA replication (*9*–*11*). Unfortunately, on the clinical aspect, LPV/r failed to demonstrate clinical benefits in well-powered randomized controlled trials (RCTs), while HCQ and/or AZ also failed to demonstrate benefits in observational studies (*12*–*14*). Meanwhile, LPV/r, CQ/HCQ and AZ may even increase the incidence of adverse events (*14*–*16*). Although remdesivir is widely considered one of the most promising candidates, latest RCTs only revealed marginal shortening of disease duration in patients treated (*17*). Therefore, further efforts are required to search for more potent, readily repurposable therapeutic agents for SARS-CoV-2 infection, either as sole therapy or im combination with other drugs to enhance their efficacy.

Ideally, the candidate drugs need to be readily available as intravenous and/or oral formulation(s), possess favourable pharmacokinetics properties as anti-infectives, and do not cause adverse events during the treatment of SARS-CoV-2 infection (e.g. non-specific immunosuppression, arrhythmia or respiratory side effects). Two complementary approaches have been adopted to identify novel drugs or compounds that can suppress SARS-CoV-2 replication. One approach relies on *in vitro*

profiling of the antiviral efficacy of up to thousands of compounds in early clinical development, or drugs already approved by the U.S. Food and Drug Administration (FDA) (*18–22*). On the other hand, as the crystal structure of the M^{pro} (*23*, *24*), papain-like protease (PL^{pro}) (*25*) and the cryo-EM structure of the nsp12-nsp7-nsp8 RdRP complex (*11*, *26*) of the SARS-CoV-2 virus became available, the structure-based development of their specific inhibitors becomes feasible. Structure-aided screening will enable the discovery of novel compounds as highly potent inhibitors (*27*) as well as the repurposing of readily available drugs as anti-CoV agents for fast-track clinical trials.

Here we report our results regarding the discovery of FDA-approved drugs potentially active against the SARS-CoV-2. *In vitro* and cellular results led to the identification of simeprevir, a hepatitis C virus (HCV) NS3A/4 protease inhibitor (*28*), as a potent inhibitor of SARS-CoV-2 replication in a cellular model of infection. Importantly, simeprevir acts synergistically with remdesivir, whereby the effective dose of remdesivr could be lowered by multiple-fold by simeprevir at physiologically feasible concentrations. Interestingly, biochemical and molecular characterizations revealed that simeprevir only weakly inhibits M^{pro}, while no inhibition of either the PL^{pro} or the RdRP polymerase activity was found. The anti-SARS-CoV-2 mechanism of simeprevir thus awaits further investigations and may provide hints on novel antiviral strategies.

Results

A prioritized screening identified simeprevir as a potent suppressor of SARS-CoV-2 replication in a cellular infection model

Given our goal of identifying immediately usable and practical drugs against SARS-CoV-2, we prioritized a list of repurposing drug candidates for *in vitro* testing based on joint considerations on safety, pharmacokinetics, drug formulation availability, and feasibility of rapidly conducting trials (**Table S1**). We focused on FDA-approved antivirals (including simeprevir, saquinavir, daclatasvir, ribavirin, sofosbuvir and zidovudine), and drugs whose primary indication was not antiviral but had reported antiviral activity (including bromocriptine and atovaquone). Remdesivir was also tested for comparison of efficacy and as a positive control.

In the Vero E6 cellular infection model, we found simeprevir as the only drug among our prioritized candidates that showed potent suppression of SARS-CoV-2 replication in the ≤ 10 μM range (**Fig. 1A**). More detailed dose-response characterization found simeprevir has a potency comparable to remdesivir in our experiment (**Fig. 1B**). The half-maximal effective concentration (EC_{50}) of simeprevir was determined to be 4.08 μM, while the 50% cytotoxicity concentration (CC_{50}) was 19.33 μM, which the latter is consistent with previously reported values in other human cell lines (*29*) (**Fig. 1B**). These data suggest that a desirable therapeutic window exists for the suppression of SARS-CoV-2 replication with simeprevir.

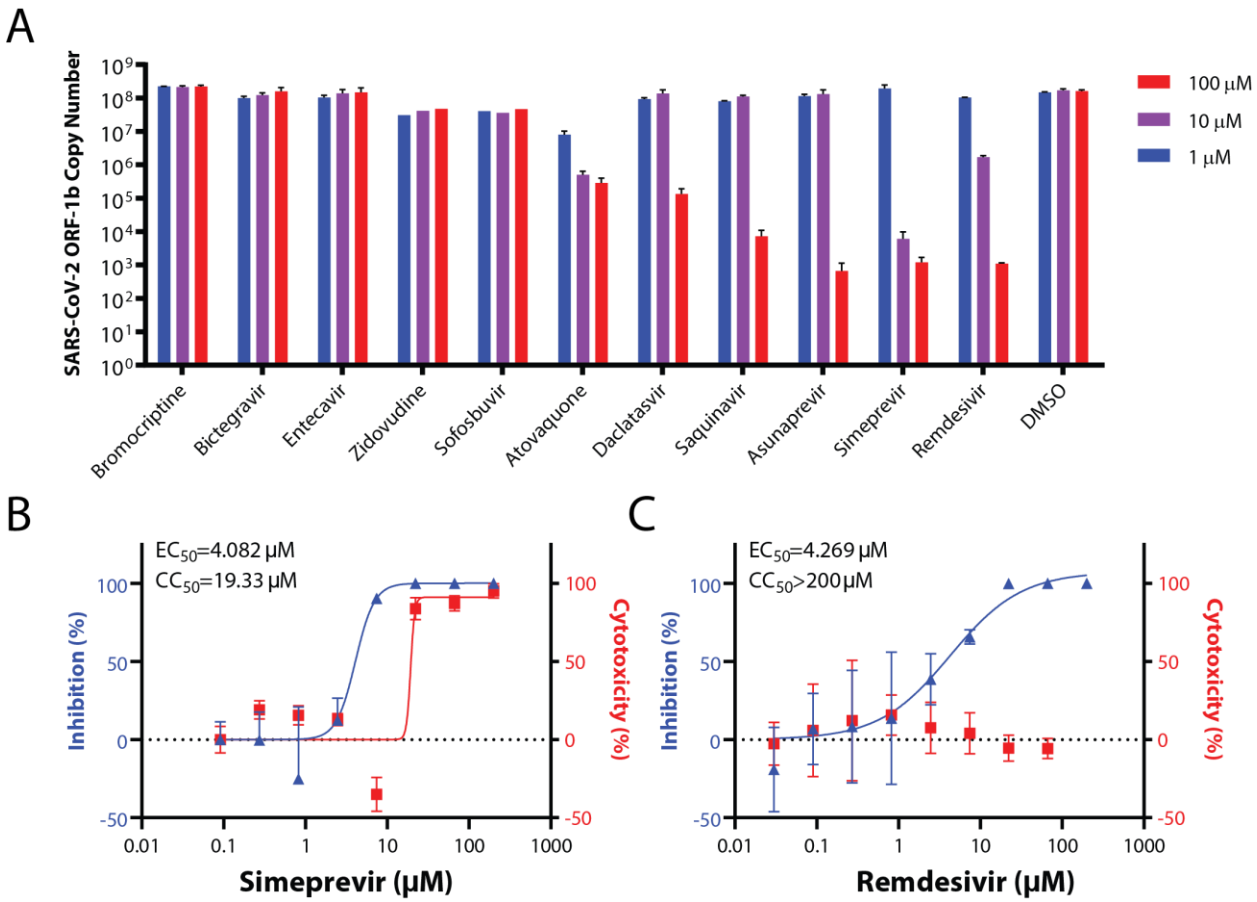

Fig. 1 (A) Screening for FDA-approved small molecule therapeutics for activities in suppressing SARS-CoV-2 replication in Vero E6 cells. Dose-response curves in the suppression of SARS-CoV-2 replication in Vero E6 cells and cytotoxicity for simeprevir **(B)** and remdesivir **(C)** are shown.

Simeprevir potentiates the suppression of SARS-CoV-2 replication by remdesivir

While simeprevir is a potential candidate for clinical use alone, we hypothesized that it may be used to create a synergistic effect with remdesivir, thereby mitigating its reported adverse effects (*17*), improving its efficacy and broadening its applicability. Indeed, combining simeprevir and remdesivir at various concentrations apparently provided much greater suppression of SARS-CoV-2 replication than remdesivir alone, while they did not synergize to increase cytotoxicity (**Fig. 2A**). Importantly, such effects were not merely additive, as the excess over Bliss score suggested synergism at 3.3 μM simeprevir and 1.1 – 10 μM remdesivir in suppressing SARS-CoV-2 replication (**Fig. 2B**).

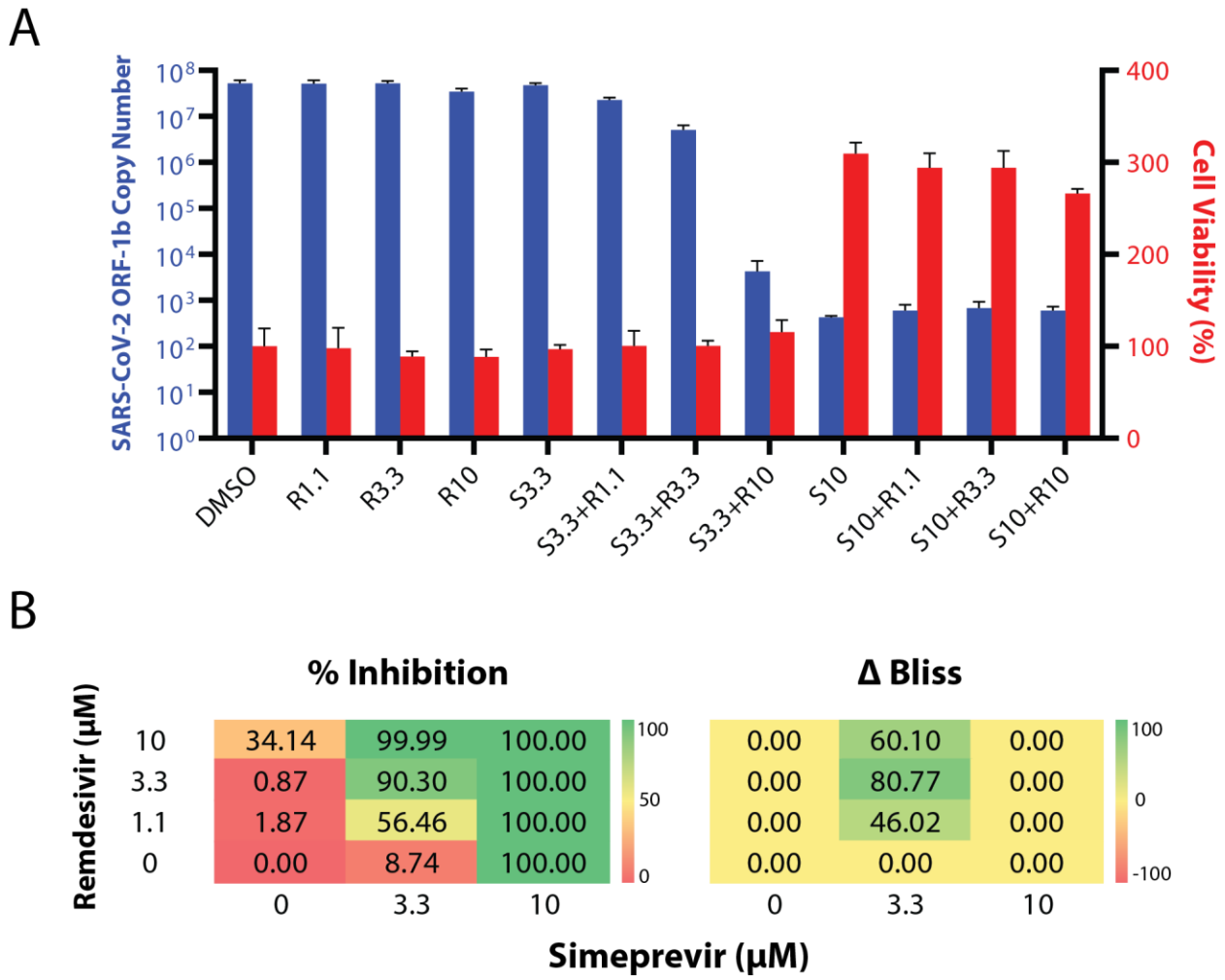

Fig. 2 (A) Viral replication-suppression efficacies of different combinations of simeprevir and remdesivir concentrations. The number behind S (simeprevir) and R (remdesivir) indicate the respective drug concentrations in μM. **(B)** Bliss score analyses of synergism. Left panel: Diagram showing 12 combinations of simeprevir and remdesivir and their respective percentage inhibition (% inhibition, color-coded) of SARS-CoV-2 replication in Vero E6 cells compared to DMSO controls. Right panel: Excess over Bliss score (ΔBliss, color-coded) of different drug combinations. A positive and negative number indicates a likely synergistic and antagonistic effect, respectively, while a zero value indicates independency.

Simeprevir weakly inhibits the SARS-CoV-2 M^{Pro} but does not inhibit PL^{pro} or RdRP at physiologically feasible concentrations

The desirable anti-SARS-CoV-2 effect of simeprevir prompted us to determine its mechanism of action. Given that simeprevir is an HCV NS3/4A protease inhibitor, we first investigated its inhibitory activity against SARS-CoV-2 M^{pro} and PL^{pro} using established *in vitro* assays (*30*, *31*) (**Fig. 3A, C, E**). We found inhibition of M^{pro} by simeprevir with half-maximal inhibitory concentration (IC_{50}) of 9.6 ± 2.3 μM (**Fig. 3B**), two times higher than the EC_{50} determined from our cell-based assay. The substrate cleavage was further verified with SDS-PAGE (**Supplementary Fig. 2**). Docking simeprevir against the apo protein crystal structure of SARS-CoV-2 M^{pro} (PDB ID 6YB7; resolution: 1.25 Å) suggested a putative binding mode with a score of -9.9 kcal mol^{-1} (**Supplementary Fig. 3**). This binding mode is consistent with a recent docking study using a homology model of SARS-CoV-2 M^{pro} (*32*). On the other hand, no inhibition of PL^{pro} activity was observed even at above 20 μM of simeprevir (**Fig. 3D**).

We speculated that the weak inhibition of M^{pro} protease activity by simeprevir could not fully account for its antiviral effect towards SARS-CoV-2. To search for further mechanistic explanations, we

next docked simeprevir, alongside several other drug candidates, and nucleoside analogues (remdesivir, ribavirin and favipiravir) against the motif F active site of the cryo-EM structure of the SARS-CoV-2 nsp12 RdRP (**Supplementary Fig. 4A**). Interestingly, the docking results revealed that simeprevir had a higher score than the nucleoside analogues (**Supplementary Fig. 4B**). To test this experimentally, we adopted previously reported protocols and constructed an RdRP primer extension assay using recombinant SARS-CoV-2 nsp12, nsp7 and nsp8. Intriguingly, simeprevir showed no inhibition of RdRP polymerase activity at concentrations as high as 500 μM (**Fig. 3F**). Since simeprevir only weakly inhibits M^{pro} and does not inhibit the enzyme activities of SARS-CoV-2 RdRP or PL^{pro} *in vitro*, it may function by targeting other host or viral protein(s).

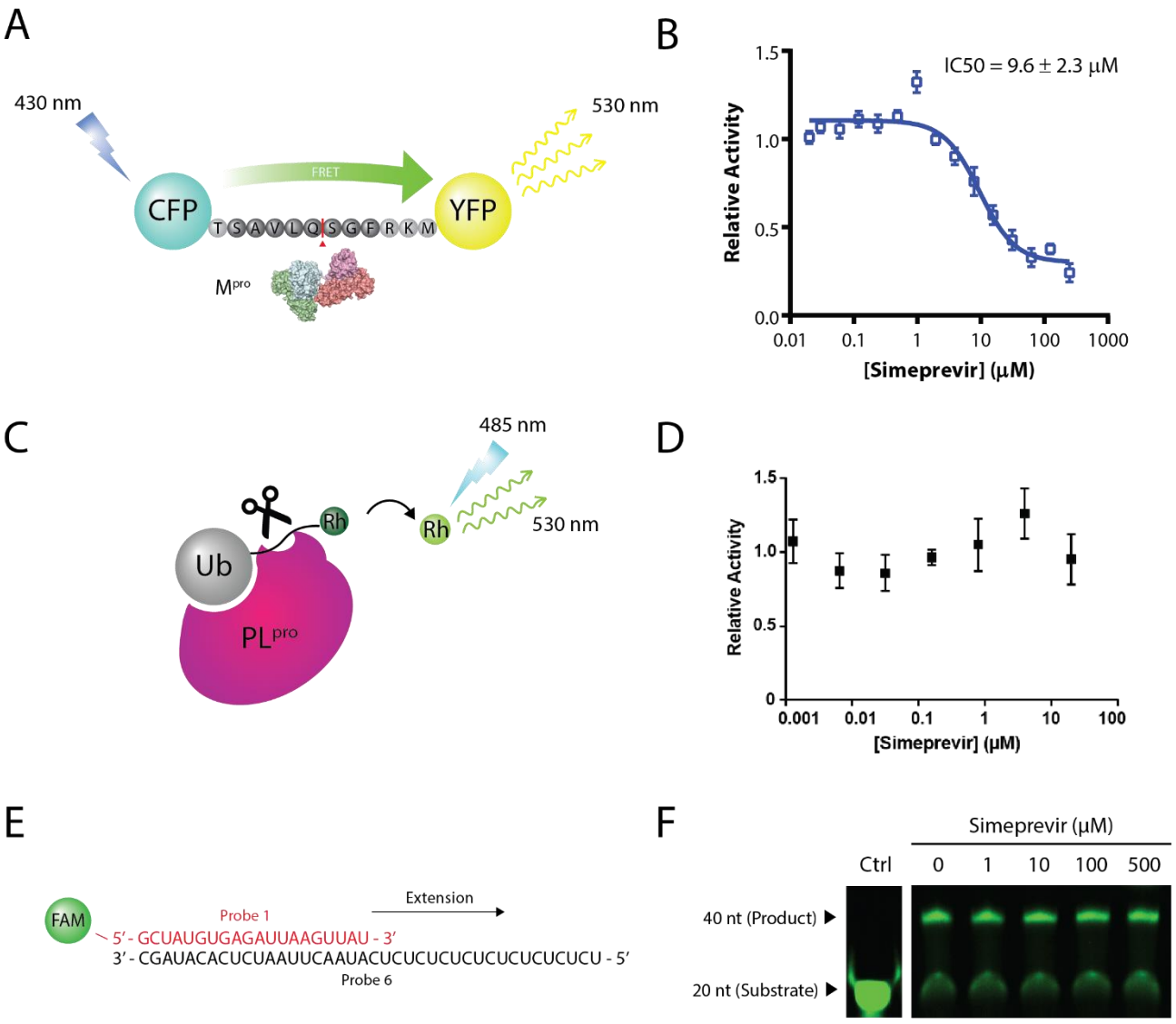

Fig. 3 Inhibitory activity of various viral proteins by Simeprevir. (A) Assay scheme of SARS-CoV-2 main protease (M^{pro}). **(B)** Inhibition of SARS-CoV-2 M^{pro} protease activity by simeprevir in a FRET-based assay with an IC_{50} of 9.6 ± 2.3 μM. **(C)** Assay scheme of SARS-CoV-2 papain-like protease (PL^{pro}). **(D)** No inhibition of SARS-CoV-2 PL^{pro} activity by simeprevir at concentrations up to 20 μM. **(E)** Assay scheme of SARS-CoV RNA-dependent RNA polymerase (RdRP) activity. **(F)** No inhibition of SARS-CoV-2 RdRP polymerase activity by simeprevir in a primer extension assay at concentrations up to 500 μM.

Discussion

The SARS-CoV-2 has gone from an emerging infection to a global pandemic as a novel pathogen with high transmissibility. It is essential to reduce the casualties by effective pharmacological management. Our study has successfully identified the readily repurposable, clinically practical antiviral simeprevir that could target SARS-CoV-2. Specifically, we found a fourth-order suppression of viral genome copies by simeprevir at ≤ 10 μM in a cell-based viral replication assay - a concentration that is expected to be attainable in human lung tissues with ≥ 150mg daily dosing based on available pharmacokinetic data (*33*, *34*).

In addition, we discovered that simeprevir can synergize with remdesivir in inhibiting SARS-CoV-2 replication in a cellular model, potentially allowing lower doses of both drugs to be used to treat COVID-19. In a global pandemic with patients having diverse clinical characteristics, providing an additional option to remdesivir and the flexibility of combined simeprevir-remdesivir use will be exceptionally important to treat those who are intolerant or not responding to the drug (*17*), which can easily amount to tens of thousands of patients given the widespread disease. As there is only one confirmed and approved therapy for COVID-19, a potentially repurposable drug can be rapidly tested in animal models before clinical trials to prepare for supply shortages or when remdesivir-resistant mutations arise.

We note, however, there are also several disadvantages of simeprevir and the proposed simeprevir-remdesivir combination. Simeprevir requires dose adjustments in patients with Child-Pugh Class B or C cirrhosis, as well as in patients with East Asian ancestry (*33*). In addition, simeprevir has been taken off the market since 2018 due to the appearance of next-generation HCV protease inhibitors, hence its supply may not be ramped up easily. As simeprevir is only available in an oral capsule formulation, it cannot be easily administered in the most severe patients who may be intubated. Finally, simeprevir is metabolized by the CYP3A4 enzyme with saturable kinetics (*33*) while remdesivir itself is not only a substrate of CYP3A4 and esterases but also a CYP3A4 inhibitor. Whether such theoretical pharmacokinetic interaction will exacerbate liver toxicity or provide additional pharmacokinetic synergy (in addition to pharmacodynamic synergy) *in vivo* remains to be tested.

Mechanistically, we found unexpected complexity in the inhibition of SARS-CoV-2 replication by simeprevir - it does not inhibit the SARS-CoV-2 viral proteins PL^{pro} or RdRP at physiologically feasible concentrations. Simeprevir is a weak inhibitor of M^{pro} at ~10 μM, in keeping with the IC_{50} at ~13.7 μM as determined in a parallel study (*31*). This potency of M^{pro} inhibition unlikely accounts for the strong suppression of SARS-CoV-2 viral replication observed. Therefore, further investigation of the mechanism of action of simeprevir can uncover new druggable targets for inhibiting SARS-CoV-2 replication.

Materials and Methods

Chemicals and reagents

Bromocriptine Mesylate (BD118791), Saquinavir (BD150839), Bictegravir (BD767657), Atovaquone (BD114807) and Asunaprevir (BD626409) were purchased from BLD Pharmatech (Shanghai, China). Entecavir (HY-13623), Zidovudine (HY-17413), Sofosbuvir (HY-15005), Daclatasvir (HY-10466), Simeprevir (HY-10241) Remdesivir (HY-104077) and Remdesivir triphosphate sodium

(HY-126303A) were purchased from MedChemExpress (Monmouth Junction, NJ). Drug stocks were made with DMSO.

In vitro SARS-CoV-2 antiviral tests

SARS-CoV-2 virus (BetaCoV/Hong Kong/VM20001061/2020, SCoV2) was isolated from the nasopharynx aspirate and throat swab of a COVID-19 patient in Hong Kong using Vero E6 cells (ATCC CRL-1586). Vero E6 cells were infected with SCoV2 at a multiplicity of infection (MOI) of 0.05 in the presence of varying concentrations and/or combinations of the test drugs. DMSO as the vehicle was used as a negative control. Antiviral activities were evaluated by quantification of SARS-CoV-2 ORF1b copy number in the culture supernatant by using quantitative real-time RT-PCR (qPCR) at 48 h post-infection with specific primers targeting the SARS-CoV-2 ORF1b (*35*).

Molecular docking simulations

Three-dimensional representations of chemical structures were extracted from the ZINC15 database (http://zinc15.docking.org) (*36*), with the application of three selection filters — Protomers, Anodyne, and Ref. ZINC15 subset DrugBank FDA (http://zinc15.docking.org./catalogs/dbfda/) were downloaded as the mol2 file format. The molecular structures were then converted to the pdbqt format (the input file format for AutoDock Vina) using MGLTools2-1.1 RC1 (sub-program “prepare_ligand”) (http://adfr.scripps.edu/versions/1.1/downloads.html). AutoDock Vina v1.1.2 was employed to perform docking experiments (*37*). Docking of simeprevir on SARS-CoV-2 M^{pro} was performed with the target structure based on an apo protein crystal structure (PDB ID: 6YB7); the A:B dimer was generated by crystallographic symmetry. Docking was run with the substrate-binding residues set to be flexible. Docking of simeprevir and other active triphosphate forms of nucleotide analogues was performed against the nsp12 portion of the SARS-CoV-2 nsp12-nsp7-nsp8 complex cryo-EM structure (PDB ID: 6M71).

Expression and purification of M^{pro} and its substrate for FRET assay

The sequence of SARS-CoV-2 M^{pro} was obtained from GenBank (accession number: YP_009725301), codon-optimized, and ordered from GenScript. A C-terminal hexahistidine-maltose binding protein (His_6-MBP) tag with two in-between Factor Xa digestion sites were inserted. Expression and purification of SARS-CoV-2 M^{pro} was then performed as described for SARS-CoV M^{pro} (*30*). The protein substrate, where the cleavage sequence “TSAVLQSGFRKM” of M^{pro} was inserted between a cyan fluorescent protein and a yellow fluorescent protein, was expressed and purified as described (*30*).

In vitro M^{pro} inhibition assay

The inhibition assay was based on fluorescence resonance energy transfer (FRET) using a fluorescent-protein-based substrate previously developed for SARS-CoV M^{pro} (*30*, *38*). 0.1 μM of purified SARS-CoV-2 M^{pro} was pre-incubated with 0 - 250 μM simeprevir in 20 mM HEPES pH 6.5, 120 mM NaCl, 0.4 mM EDTA, 4 mM DTT for 30 min before the reaction was initiated by addition of 10 μM protein substrate (*31*). Protease activity was followed at 25 °C by FRET with excitation and emission wavelengths of 430 nm and 530 nm, respectively, using a multi-plate reader as described (*30*, *38*). Reduction of fluorescence at 530 nm was fitted to a single exponential decay to obtain the observed

rate constant (k_{obs}). Relative activity of M^{pro} was defined as the ratio of k_{obs} with inhibitors to that without. The relative IC_{50} value of simeprevir was determined by fitting the relative activity at different inhibitor concentration to a four-parameter logistics equation.

Expression and purification of nsp7, nsp8, nsp12

The nsp7 and nsp8 genes were retrieved from GenBank (accession number:YP_009725303.1 & YP_009725304.1) N-terminally hexahistidine-tagged, codon-optimized, and chemically synthesized and cloned into the vector pET-45b(+) (GeneScript). The plasmids were separately transformed into *Escherichia coli* BL21 (DE3) competent cells and grown in 2YT media supplemented with 100 µg/ml ampicillin at 37 °C. When the OD_{600} of the cells reached 0.8, expression was induced with 1 mM isopropyl β-D-1-thiogalactopyranoside (IPTG) and the cells were grown at 16 °C overnight. The cells were harvested by centrifugation at 6238 × g for 10 min at 4 °C. The cell pellets for nsp7 and nsp8 were resuspended in lysis buffer [20 mM Tris (pH 7.5), 500 mM NaCl, 10 mM imidazole, 5% (v/v) glycerol, 17.4 µg/ml phenylmethylsulfonyl fluoride (PMSF) and 5 mM β-mercaptoethanol (BME)]. The resuspended cells were lysed by sonication and the lysates were separated from the insoluble fractions by centrifugation at 24,000 rpm (69,673 x g) for 30 min at 4°C. The proteins were purified by nickel affinity using a His-trap column (GE Healthcare) equilibrated with lysis buffer. The column was washed with 10 column volumes of wash buffer (20 mM Tris (pH 7.5), 500 mM NaCl, 40 mM imidazole, 5% glycerol and 5 mM BME) and the proteins were eluted with 3 - 4 column volumes of elution buffer (20 mM Tris (pH 7.5), 500 mM NaCl, 500 mM imidazole, 5% glycerol and 5 mM BME). The eluted proteins were further purified by size exclusion chromatography using a Superdex 200 16/600 column (GE Healthcare) equilibrated with a buffer containing 25 mM Tris (pH 7.5), 300 mM NaCl, 0.1 mM $MgCl_2$ and 1 mM dithiothreitol (DTT). The relevant protein fractions were pooled, concentrated to 7.93 mg/ml (nsp7) and 93 mg/ml (nsp8) respectively, and stored at -80 °C.

The nsp12 protein was purchased from GenScript. Briefly, the gene sequence for SARS-CoV-2 nsp12 was retrieved from GenBank [Accession Number: QHD43415.1(4393...5324)], codon-optimized for Sf9 insect cells and chemically synthesized (GenScript). The DNA fragment was then subcloned into pFastBac1 using EcoRI/HindIII with a 5' Kozak sequence, C-terminal thrombin site and hexahistidine tag, adding additional amino acids MGLQ to the N-terminus and LVPRGSGHHHHHH to the C-terminus of the protein. The plasmids were amplified in *E. coli* TOP10 cells and transformed into *E. coli* DH10Bac cells (Life Technologies) for bacmid production. The nsp12 bacmids were transfected into Sf9 cells (Expression Systems) using transfection Reagent FuGENE® 6 (Promega). The recombinant baculovirus was amplified twice in Sf9 cells. 10 mL of the second amplification was used to infect 1 L of Sf9 cells at 3 × 106 cells/mL and incubated at 27 °C for 48 h. Cells were harvested by centrifugation at 1000 × g and resuspended in 70 mL of Lysis Buffer (25 mM HEPES pH 7.4, 300 mM NaCl, 1 mM $MgCl_2$, 2 mM DTT). The resuspended cells were then mixed with an equal volume of lysis buffer containing 0.2% (v/v) Igepal CA-630 (Anatrace) and incubated with agitation for 10 min at 4 °C. The cell lysate was then sonicated before clarification by centrifugation at 15,000 × g at 4 °C for 30 min. Cleared lysates were incubated with Ni-NTA beads for 2 h (GenScript), washed with Lysis buffer, and eluted with Lysis buffer containing step gradients of 20 – 500 mM imidazole. The eluted protein was dialysed against protein storage buffer (25 mM HEPES pH 7.5, 300 mM NaCl, 0.1 mM $MgCl_2$, 2 mM TCEP), concentrated with Amicon Ultra concentrator (Millipore Sigma), and stored at -80 °C.

In vitro RdRP inhibition assay

For nsp12-nsp7-nsp8 complex formation, 5 μM of purified SARS-CoV-2 nsp12 was mixed with separately purified nsp7 and nsp8 in 1:6:6 molar ratio in RdRP assay buffer (25 mM Tris-HCl pH 7.5, 300 mM NaCl, 0.1 mM $MgCl_2$, 1 mM DTT) and incubated at 4 °C overnight. For the RNA template (ordered from General Biosystems), 5' FAM labelled RNA probe 1 (5'-GCUAUGUGAGAUUAAGUUAU-3') and unlabelled RNA probe 6 (5'-UCUCUCUCUCUCUCUCUCUCAUAACUUAAUCUCACAUAGC-3') were mixed in 1:1 molar ratio to a final concentration of 40 μM each in RNA annealing buffer (20 mM Tris-HCl pH 8, 50 mM NaCl, 5 mM EDTA), denatured at 95 °C for 5 min and cooled to 25 °C over the course of 10 min in a thermocycler. To test the activity of the recombinant nsp12-nsp7-nsp8 complex, 4 μM of the protein complex was incubated at 27 °C for 1 h in the presence of 1 μM RNA template, 0.5 U/μL SuperaseIn (Thermo Fisher) and 50 μM NTP in RdRP assay buffer. For Simeprevir inhibitory assay, different concentrations of Simeprevir in DMSO were added to the reaction mixture, comprising 5% of the reaction volume. Reactions were terminated by addition of equal volume 2x RNA loading buffer (0.5x Gel Loading Dye Purple (NEB) in 90% formamide), denatured at 95 °C for 5 min and immediately transferred on ice. Reaction products were analyzed on 8M Urea, 15% polyacrylamide (acrylamide:bis-acrylamide = 19:1) minigel buffered with 1X TBE. After running at 250 V for 25 min, the gel was imaged with Gel Doc EZ Imager (Bio-Rad) using the Ethidium Bromide mode.

In vitro PL^{pro} inhibition assay

The purification and assay of PL^{pro} activity was adapted from as previously described (*25*). Briefly, a ubiquitin protein tagged with rhodamine-modified PL^{pro} cleavage site was used as a substrate for the enzymatic assay. 5 uL of solution containing 0 - 20 μM of Simeprevir and 10 μM of ubiquitin-rhodamine were aliquoted into a 384-well plate. Reaction was initiated by addition of 5 μL of 30 nM PL^{pro} to the well. Initial velocities of rhodamine release were normalized against DMSO control. Reactions were conducted for 300 seconds with monitoring of fluorescence intensity at 485/520 nm using a microplate reader (PHERAstar FSX, BMG Labtech).

Acknowledgments: We thank Dr. Martin Chan (CUHK) for helpful discussions during the early phase of this project. We thank Ms. Diana Grewe for technical assistance. We also thank Prof. Vincent Lee (CUHK) and Dr. Ivanhoe Leung (University of Auckland) for the critical comments on this manuscript.

Funding: W.L.N. acknowledges funding support from CUHK (the "Improvement on competitiveness in hiring new faculties funding scheme" and a seed fund from the Faculty of Medicine) and the Croucher Foundation (start-up fund). W.S.A. acknowledges HKBU's funding support through the Tier2 Start-up Grant (RC-SGT2/18-19/SCI/003).

Author contributions: W.L.N. & M.C.W.C. oversaw the project. H.S.L., H.M.L., H.K., & W.L.N. wrote the manuscript with input from all authors. K.P.Y.H., K.C.N. & J.C.W.H. contributed to the viral infection assay. H.S.L., S.K., H.M.L., B.M. & W.S.A. contributed to the development of the RdRp assay. K.S.K., H.H.Y.C. & K.B.W. contributed to the development of the 3CLPro assay. D.S., K.P.W., I.D. & P.H.L. contributed to the development of the PLP assay. K.W. contributed to protein expression and purification. H.S.L., A.K.N.C., Y.W.C. & P.M.H.C. contributed to molecular modeling. Z.L. contributed to the mechanistic study. H.M.L., Z.Z., F.K.L.C., D.S.C.H., V.C.T.M. H.K., M.C.W.C. & W.L.N. contributed to the conceptual design of the project.

Competing interests: CUHK and HKU have filed a US provisional patent application based on the finding of this manuscript. W.L.N., M.C.W.C., K.P.Y.H., H.S.L., K.S.K., H.K. and H.M.L. are inventors of the patent. F.K.L.C. has served as a consultant to Eisai, Pfizer, Takeda and Otsuka, and has been paid lecture fees by Eisai, Pfizer, AstraZeneca and Takeda.

Data and materials availability: The raw data and data analysis codes used in this project are available from the authors upon reasonable request.

References:

1. C. Huang *et al.*, Clinical features of patients infected with 2019 novel coronavirus in Wuhan, China. *Lancet*. 395, 497–506 (2020).

2. N. Chen *et al.*, Epidemiological and clinical characteristics of 99 cases of 2019 novel coronavirus pneumonia in Wuhan, China: a descriptive study. *Lancet*. 395, 507–513 (2020).

3. F. Zhou *et al.*, Clinical course and risk factors for mortality of adult inpatients with COVID-19 in Wuhan, China: a retrospective cohort study. *Lancet*. 395, 1054–1062 (2020).

4. W.-J. Guan *et al.*, Clinical characteristics of coronavirus disease 2019 in China. *N. Engl. J. Med.* (2020), doi:10.1056/NEJMoa2002032.

5. R. Li *et al.*, Substantial undocumented infection facilitates the rapid dissemination of novel coronavirus (SARS-CoV-2). *Science*. 368, 489–493 (2020).

6. J. M. Sanders, M. L. Monogue, T. Z. Jodlowski, J. B. Cutrell, Pharmacologic Treatments for Coronavirus Disease 2019 (COVID-19): A Review. *JAMA* (2020), doi:10.1001/jama.2020.6019.

7. K. A. Pastick *et al.*, Review: Hydroxychloroquine and Chloroquine for Treatment of SARS-CoV-2 (COVID-19). *Open Forum Infect. Dis.* 7, ofaa130 (2020).

8. A. Zumla, J. F. W. Chan, E. I. Azhar, D. S. C. Hui, K.-Y. Yuen, Coronaviruses - drug discovery and therapeutic options. *Nat. Rev. Drug Discov.* 15, 327–347 (2016).

9. T. P. Sheahan *et al.*, An orally bioavailable broad-spectrum antiviral inhibits SARS-CoV-2 in human airway epithelial cell cultures and multiple coronaviruses in mice. *Sci. Transl. Med.* 12 (2020), doi:10.1126/scitranslmed.abb5883.

10. C. J. Gordon *et al.*, Remdesivir is a direct-acting antiviral that inhibits RNA-dependent RNA polymerase from severe acute respiratory syndrome coronavirus 2 with high potency. *J. Biol. Chem.* (2020), doi:10.1074/jbc.RA120.013679.

11. W. Yin *et al.*, Structural basis for inhibition of the RNA-dependent RNA polymerase from SARS-CoV-2 by remdesivir. *Science* (2020), doi:10.1126/science.abc1560.

12. E. S. Rosenberg *et al.*, Association of Treatment With Hydroxychloroquine or Azithromycin With In-Hospital Mortality in Patients With COVID-19 in New York State. *JAMA* (2020), doi:10.1001/jama.2020.8630.

13. J. Geleris *et al.*, Observational Study of Hydroxychloroquine in Hospitalized Patients with Covid-19. *N. Engl. J. Med.* (2020), doi:10.1056/NEJMoa2012410.

14. B. Cao *et al.*, A Trial of Lopinavir-Ritonavir in Adults Hospitalized with Severe Covid-19.

N. Engl. J. Med. 382, 1787–1799 (2020).

15. K. Gbinigie, K. Frie, Should chloroquine and hydroxychloroquine be used to treat COVID-19? A rapid review. *Br J Gen Pract Open* (2020), doi:10.3399/bjgpopen20X101069.

16. E. Chorin *et al.*, QT Interval Prolongation and Torsade De Pointes in Patients with COVID-19 treated with Hydroxychloroquine/Azithromycin. *Heart Rhythm* (2020), doi:10.1016/j.hrthm.2020.05.014.

17. Y. Wang *et al.*, Remdesivir in adults with severe COVID-19: a randomised, double-blind, placebo-controlled, multicentre trial. *Lancet* (2020), doi:10.1016/S0140-6736(20)31022-9.

18. M. Ko, S. Jeon, W.-S. Ryu, S. Kim, Comparative analysis of antiviral efficacy of FDA-approved drugs against SARS-CoV-2 in human lung cells: Nafamostat is the most potent antiviral drug candidate. *BioRxiv* (2020), doi:10.1101/2020.05.12.090035.

19. S. Weston, R. Haupt, J. Logue, K. Matthews, M. Frieman, FDA approved drugs with broad anti-coronaviral activity inhibit SARS-CoV-2 *in vitro*. *BioRxiv* (2020), doi:10.1101/2020.03.25.008482.

20. L. Riva *et al.*, A Large-scale Drug Repositioning Survey for SARS-CoV-2 Antivirals. *BioRxiv* (2020), doi:10.1101/2020.04.16.044016.

21. M. Wang *et al.*, Remdesivir and chloroquine effectively inhibit the recently emerged novel coronavirus (2019-nCoV) in vitro. *Cell Res.* 30, 269–271 (2020).

22. K.-T. Choy *et al.*, Remdesivir, lopinavir, emetine, and homoharringtonine inhibit SARS-CoV-2 replication in vitro. *Antiviral Res.* 178, 104786 (2020).

23. L. Zhang *et al.*, Crystal structure of SARS-CoV-2 main protease provides a basis for design of improved α-ketoamide inhibitors. *Science*. 368, 409–412 (2020).

24. Z. Jin *et al.*, Structure of Mpro from SARS-CoV-2 and discovery of its inhibitors. *Nature* (2020), doi:10.1038/s41586-020-2223-y.

25. D. Shin *et al.*, Inhibition of papain-like protease PLpro blocks SARS-CoV-2 spread and promotes anti-viral immunity (2020), doi:10.21203/rs.3.rs-27134/v1.

26. Y. Gao *et al.*, Structure of the RNA-dependent RNA polymerase from COVID-19 virus. *Science*. 368, 779–782 (2020).

27. Z. Jin *et al.*, Structural basis for the inhibition of SARS-CoV-2 main protease by antineoplastic drug carmofur. *Nat. Struct. Mol. Biol.* (2020), doi:10.1038/s41594-020-0440-6.

28. Å. Rosenquist *et al.*, Discovery and development of simeprevir (TMC435), a HCV NS3/4A protease inhibitor. *J. Med. Chem.* 57, 1673–1693 (2014).

29. T.-I. Lin *et al.*, In vitro activity and preclinical profile of TMC435350, a potent hepatitis C virus protease inhibitor. *Antimicrob. Agents Chemother.* 53, 1377–1385 (2009).

30. C.-P. Chuck *et al.*, Profiling of substrate specificity of SARS-CoV 3CL. *PLoS ONE*. 5, e13197 (2010).

31. C. Ma *et al.*, Boceprevir, GC-376, and calpain inhibitors II, XII inhibit SARS-CoV-2 viral replication by targeting the viral main protease. *BioRxiv* (2020), doi:10.1101/2020.04.20.051581.

32. P. Calligari, S. Bobone, G. Ricci, A. Bocedi, Molecular Investigation of SARS-CoV-2 Proteins and Their Interactions with Antiviral Drugs. *Viruses*. 12 (2020), doi:10.3390/v12040445.

33. Janssen Pharmaceutica, Clinical pharmacology and biopharmaceutics reivew(s) (Application Number 205123Orig1s000), Center for Drug Evaluation and Research.

34. J. Snoeys, M. Beumont, M. Monshouwer, S. Ouwerkerk-Mahadevan, Mechanistic understanding of the nonlinear pharmacokinetics and intersubject variability of simeprevir: A PBPK-guided drug development approach. *Clin. Pharmacol. Ther.* 99, 224–234 (2016).

35. K. P. Y. Hui *et al.*, Tropism, replication competence, and innate immune responses of the coronavirus SARS-CoV-2 in human respiratory tract and conjunctiva: an analysis in ex-vivo and in-vitro cultures. *Lancet Respir. Med.* (2020), doi:10.1016/S2213-2600(20)30193-4.

36. T. Sterling, J. J. Irwin, ZINC 15--Ligand Discovery for Everyone. *J. Chem. Inf. Model.* 55, 2324–2337 (2015).

37. O. Trott, A. J. Olson, AutoDock Vina: improving the speed and accuracy of docking with a new scoring function, efficient optimization, and multithreading. *J. Comput. Chem.* 31, 455–461 (2010).

38. C.-P. Chuck *et al.*, Design, synthesis and crystallographic analysis of nitrile-based broad-spectrum peptidomimetic inhibitors for coronavirus 3C-like proteases. *Eur. J. Med. Chem.* 59, 1–6 (2013).

Supplementary Figures & Tables

Drug candidate	Approved indication(s)	Common/notable adverse effects	Drug formulation(s) available	Contraindications (except known hypersensitivity to the drug)
Simeprevir	Chronic HCV infection	Photosensitivity, rash, fatigue, myalgia, dyspnea	Oral	None
Daclatasvir	Chronic HCV infection	Fatigue, nausea, anemia, diarrhea	Oral	None
Saquinavir	HIV infection	Nausea, diarrhea, QT prolongation	Oral	Prolonged QT interval, Patients at risk/having complete AV block
Bromocriptine	Hyperprolactinemia, pituitary prolactinoma	Constipation, dizziness, nausea, fatigue, orthostatic hypotension, vasospasm, abdominal pain	Oral	Uncontrolled hypertension, psychosis, syncopal migraine
Asunaprevir	HIV infection	Fatigue, rash, nausea, neutropenia, anemia, deranged liver function tests	Oral	Moderate/severe hepatic impairment (Child B or C)
Bictegravir	HIV infection	Increased serum creatine kinase, deranged liver function tests, neutropenia	Oral	None
Entecavir	HBV infection	Deranged liver function tests	Oral	Moderate/severe hepatic impairment (Child B or C)
Zidovudine	HIV infection	Headache, malaise, rash, nausea, neutropenia, anemia	Oral	None
Sofosbuvir	Chronic HCV infection	Fatigue, headache, insomnia, nausea, diarrhea, anemia, myalgia, rash	Oral	None
Atovaquone	Protozoal infection or prophylaxis (*Pneumocystic jirovecii*, *Plasmodium* spp. etc)	Headache, insomnia, rash, diarrhea, myalgia, drug fever, hyponatremia, neutropenia	Oral	None
Remdesivir	COVID-19	Deranged liver function tests	Intravenous	Serum alanine transaminase ≥5x the upper-limit of normal

Table S1 FDA-approved repurposable drug candidates tested in this study.

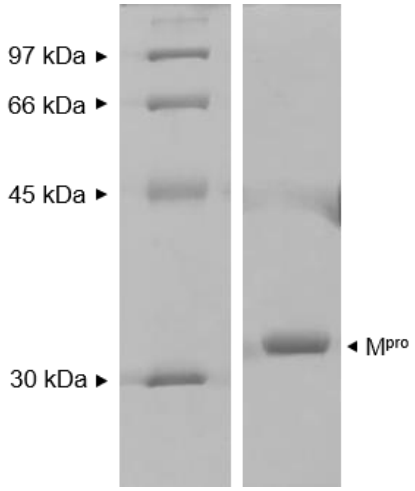

Supplementary Fig. 1 SDS-PAGE analysis of recombinant SARS-CoV-2 M^{pro}.

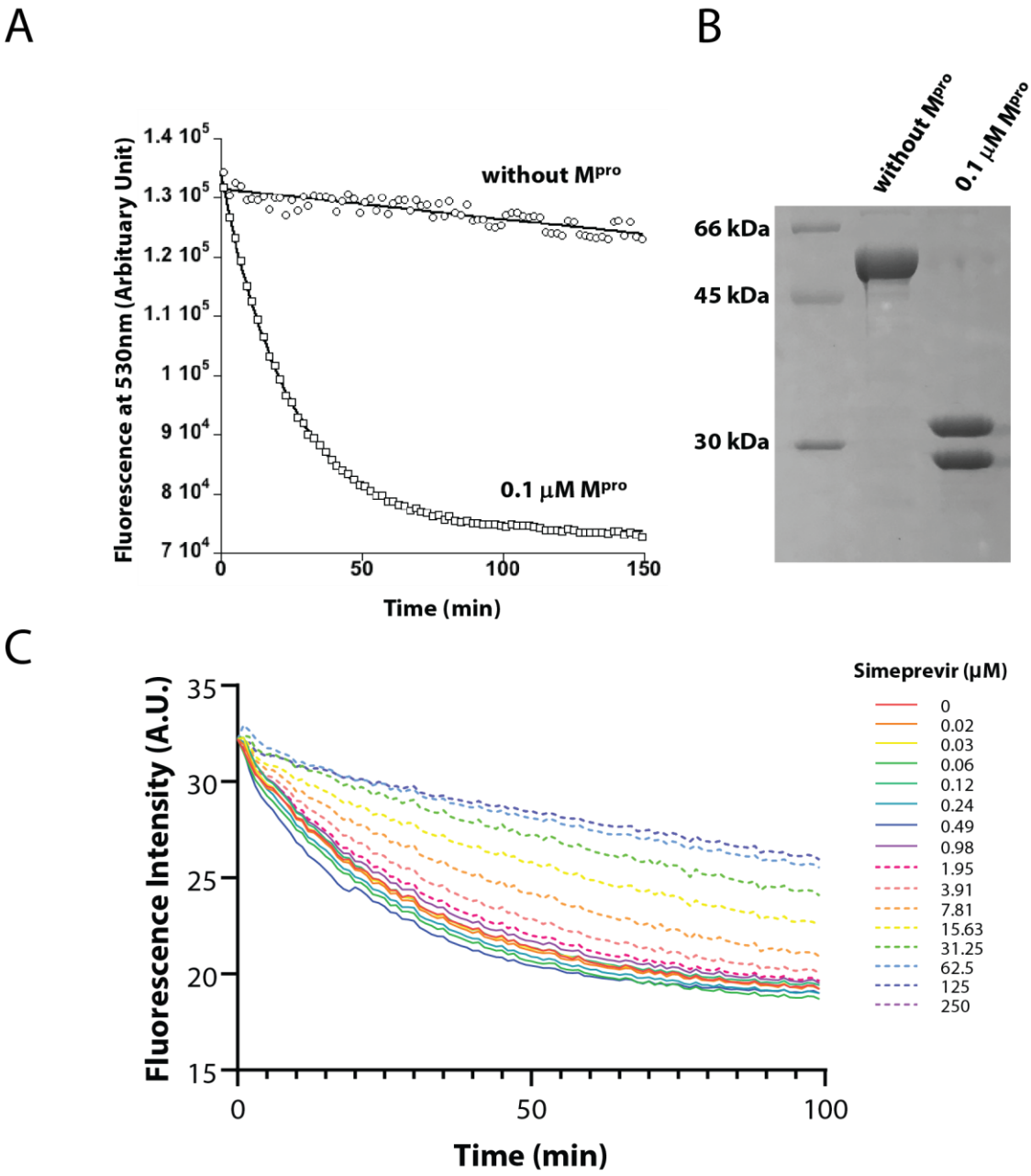

Supplementary Fig. 2 (A) The addition of SARS-CoV-2 M^{pro} led to the cleavage of the substrate, causing detectable decline in FRET signal with 430-nm excitation and 530-nm emission. **(B)** Confirmation of substrate cleavage by M^{pro} using SDS-PAGE. **(C)** The addition of simeprevir at varying concentrations attenuated the rate of FRET substrate cleavage by M^{pro}.

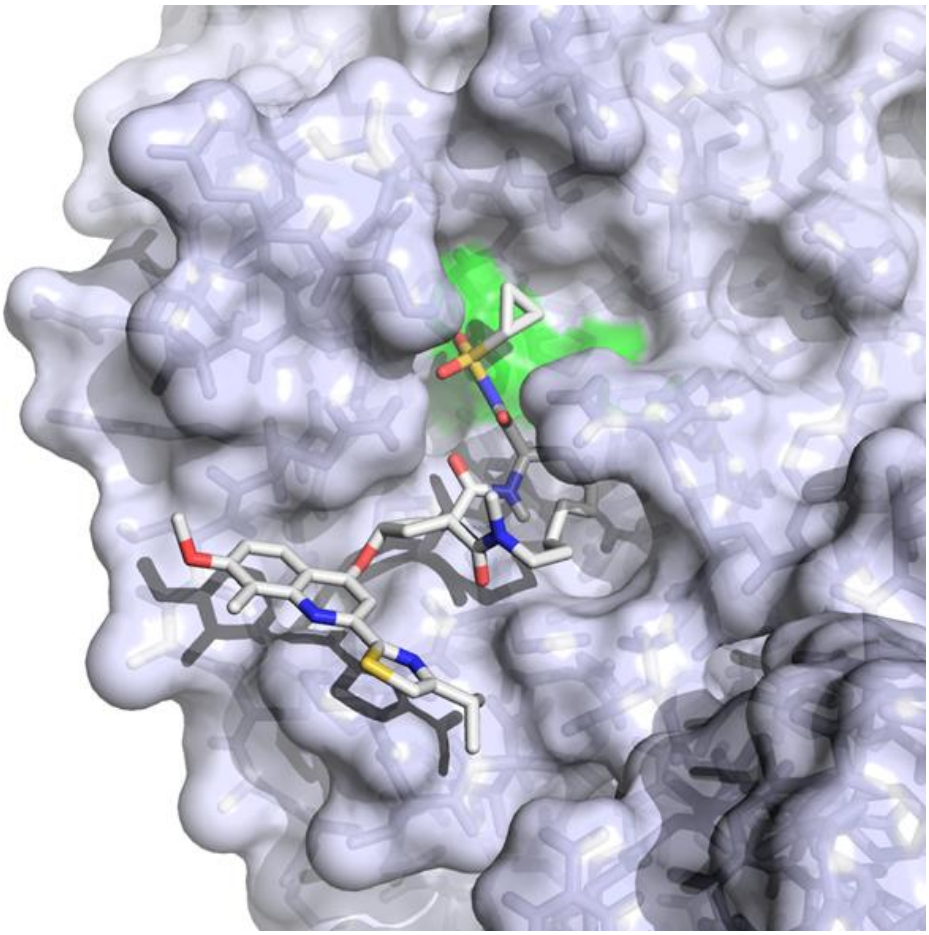

Supplementary Fig. 3 Docking of simeprevir on SARS-CoV-2 M^{pro} (performed with AutoDock Vina version 1.1.2). The M^{pro} structure was based on an apo protein crystal structure (PDB ID: 6YB7); the A:B dimer was generated by crystallographic symmetry. Docking was run with the substrate-binding residues set to be flexible; and a 30 x 30 x 30 $Å^3$ search box centered near the side-chain Nε2 atom of His163. The top docking mode shown here scored -9.9 kcal mol^{-1}. The protein is shown as a semi-transparent molecular surface encasing its stick model with the catalytic residues His41 and Cys145 in green. The ligand was shown as a stick model with oxygen atoms in red; nitrogen atoms in blue, sulfur atoms in yellow and carbon atoms in white.

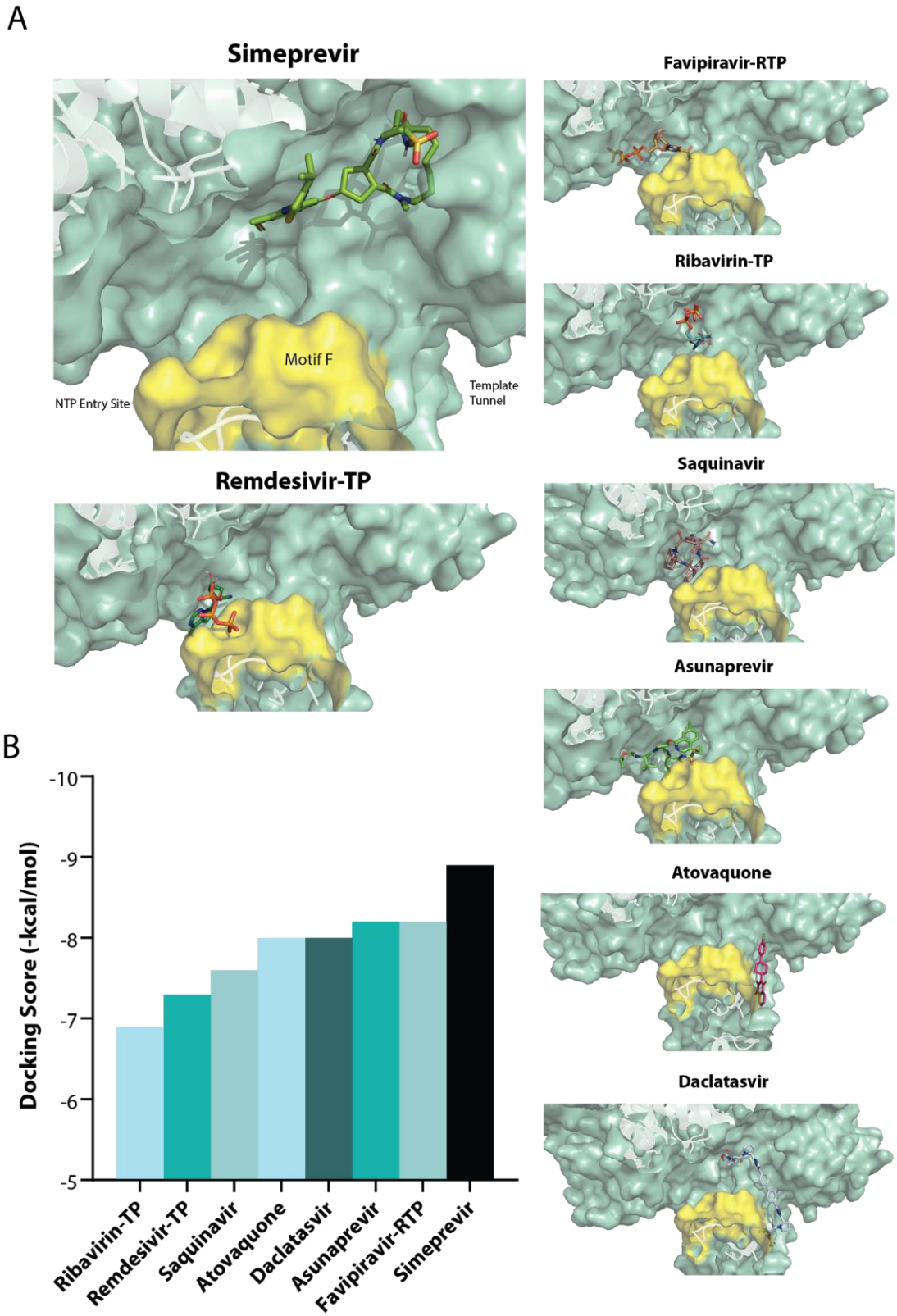

Supplementary Fig. 4 (A) Binding mode of Simeprevir and other inhibitors against SARS-CoV-2 nsp12 (PDB: 6M71). Motif F is highlighted in yellow. **(B)** Docking scores of drug candidates against nsp12.

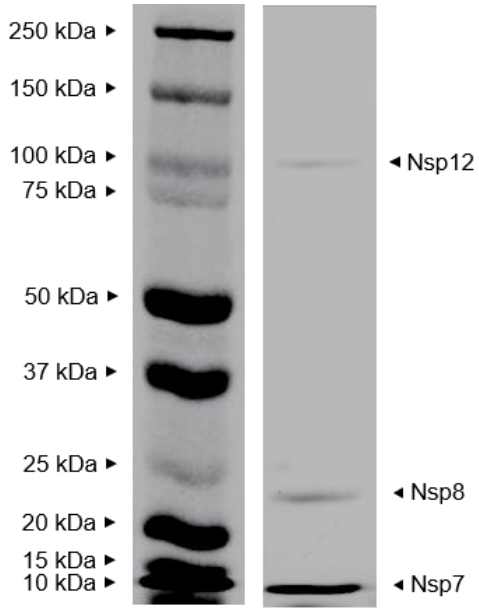

Supplementary Fig. 5 SDS-PAGE analysis of the nsp12-nsp8-nsp7 RdRP complex formed using recombinant SARS-CoV-2 proteins *in vitro*.

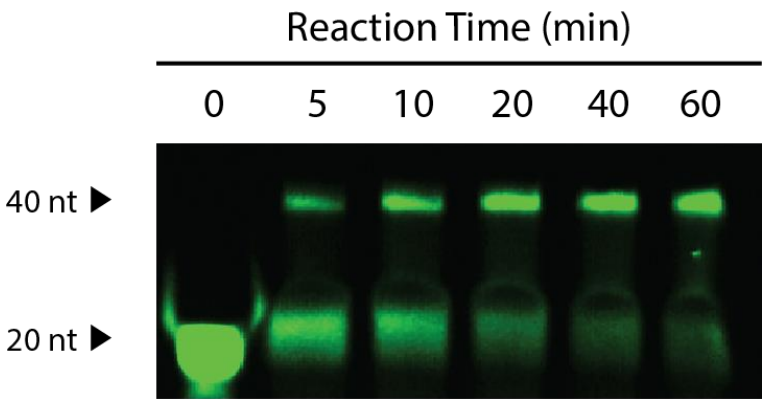

Supplementary Fig. 6 Time-dependent increase in the extension of probe 1 is apparent using urea denaturing PAGE gel analysis.